Contents lists available at ScienceDirect

Nano Energy

journal homepage: www.elsevier.com/locate/nanoenergy

Communication

Concurrent improvement in optical and electrical characteristics by using inverted pyramidal array structures toward efficient Si heterojunction solar cells

Hsin-Ping Wang [1], An-Cheng Li [1], Tzu-Yin Lin, Jr-Hau He *

Computer, Electrical and Mathematical Sciences and Engineering (CEMSE) Division, King Abdullah University of Science & Technology (KAUST), Thuwal 23955-6900, Saudi Arabia

ARTICLE INFO

Article history:
Received 12 November 2015
Received in revised form
6 February 2016
Accepted 15 February 2016
Available online 2 March 2016

Keywords:
Inverted pyramid
Photon management
Heterojunction
Solar cells

ABSTRACT

The Si heterojunction (SHJ) solar cell is presently the most popular design in the crystalline Si (*c*-Si) photovoltaics due to the high open-circuit voltages (V_{OC}). Photon management by surface structuring techniques to control the light entering the devices is critical for boosting cell efficiency although it usually comes with the V_{OC} loss caused by severe surface recombination. For the first time, the periodic inverted pyramid (IP) structure fabricated by photolithography and anisotropic etching processes was employed for SHJ solar cells, demonstrating concurrent improvement in optical and electrical characteristics (i.e., short-circuit current density (J_{SC}) and V_{OC}). Periodic IP structures show superior light-harvesting properties as most of the incident rays bounce three times on the walls of the IPs but only twice between conventional random upright pyramids (UPs). The high minority carrier lifetime of the IP structures after *a*-Si:H passivation results in an enhanced V_{OC} by 28 mV, showing improved carrier collection efficiency due to the superior passivation of the IP structure over the random UP structures. The superior antireflective (AR) ability and passivation results demonstrate that the IP structure has the potential to replace conventional UP structures to further boost the efficiency in solar cell applications.

1. Introduction

Energy harvesting in photovoltaic (PV) devices has become critical with continuous improvements in cell design for boosting cell efficiency. A lot of research efforts have focused on photon management to precisely control the light at the active layer to efficiently generate photocarriers. However, most of light-trapping schemes by employing surface structuring techniques usually accompany electrical losses (*e.g.*, carrier recombination by surface states or contact losses) [1–3]. The expected boosted short-circuit current density (J_{SC}) would be partially compromised by poor open-circuit voltages (V_{OC}) and fill factors (*FF*). Therefore, no matter what light-trapping techniques are applied on PV devices, the electrical properties need to be considered. How to optimize the trade-off between optical gain and electrical loss or even concurrently improve both optical and electrical characteristics become the most important issues for putting photon management into practice.

Heterojunction structure has been widely studied for different types of solar cells [4–7]. Generally, great solar cells must generate maximum photocarriers by broadband absorption at active region, but also assure these photo-generated carriers can be efficiently collected with minimal recombination when they travel to the terminals of the device. High recombination increases the diode saturation current, reducing the V_{OC}. By insertion of a film with wide bandgap, the carrier recombination can be efficiently reduced due to a large band offset at the heterojunction interface, leading to a higher V_{OC} [8]. Recently, the amorphous/crystalline Si (*a*-Si/*c*-Si) heterojunction solar cell structure currently is the most popular design in *c*-Si PV industries. It combines the advantages of *c*-Si solar cells with the excellent absorption and long minority carrier lifetimes and the advantage of hydrogenated *a*-Si (*a*-Si:H) with passivation characteristics [9]. The most impressive feature of this structure is its high V_{OC} which occurs due to the significant passivation effect of *a*-Si:H. Not only can the surface state density of *c*-Si be reduced, but the wide bandgap of *a*-Si:H generates a large band offset at the *a*-Si:H/*c*-Si interface, minimizing the carrier recombination loss [10]. In 2014, a world-record high efficiency among all kinds of Si-based solar cells of 25.6% was obtained with a Si heterojunction (SHJ) combined with an interdigitated back contact design [11]. According to loss analysis, the optical loss was 60–70% of the total loss [12]. By using an interdigitated back contact design, the optical loss from the metal grid electrodes and absorption of ITO on the front side can be avoided, leading to an improvement in the J_{SC} of 2.3 mA/cm^2.

* Corresponding author.
E-mail address: jrhau.he@kaust.edu.sa (J.-H. He).
[1] These authors contributed equally to this work.

http://dx.doi.org/10.1016/j.nanoen.2016.02.034
2211-2855/

J_{SC} enhancement *via* light-trapping structures is another choice to further improve the performance of SHJ solar cells. However, it is critical to design antireflective (AR) structures for SHJ solar cells. In addition to exceptional AR ability, to avoid sacrificing the high V_{OC}, it is important to well passivate the surface of solar cells. In the SHJ case, cells must be able to be well passivated by intrinsic *a*-Si:H films as thin as 5 nm. But it is difficult to employ high aspect-ratio light-trapping structures such as nanowires in SHJ solar cells because of the non-uniform coverage of *a*-Si:H and subsequent layers, which results in the degradation of the PV performance [13–18]. A random upright pyramid (UP) structure fabricated by anisotropic wet chemical etching is the most commonly used for *c*-Si-based solar cells [19–22]. However, the various sizes of random UPs with sharp pyramidal peaks do not appear to be good enough for *a*-Si:H passivation. A chemical polish treatment for structured surfaces has been developed to improve the passivation effect, but there is a corresponding decrease in the light-trapping ability [14,18,23,24]. Inverted pyramid (IP) structures, which show better light confinement than UP structures, might be a good candidate for SHJ solar cells [25–28]. Moreover, since the morphologies of IP structures are relatively uniform, without sharp peaks, they have the potential to offer better passivation results, resulting in higher V_{OC}.

Many researches only discussed the AR properties of IP structures, neglecting to look into the electrical properties after applying on practical devices. A comparison of IP structures with conventional random UP structures in SHJ devices has not yet been made. Thus, in this work, SHJ solar cells with polished, random UP and different sizes of IP surfaces are compared. The influences on the AR ability and the passivation effect of different geometric structures are investigated. It is found that the average total reflectance (R_{total}) of SHJ cells can be suppressed to less than 4.5% over a wide spectral range from 400 to 1000 nm by using the IP with 10 μm periodicity. There is a big enhancement in the J_{SC} and power conversion efficiency (CE) for IP textured SHJ solar cells (35.3 mA/cm^2 and 14.6%) compared to the random UP textured SHJ solar cells (34.2 mA/cm^2 and 12.7%). It is noteworthy that the V_{OC} of the IP textured SHJ solar cells is 28 mV higher than that of the random UPs, indicating the superior passivation of the IP structure over the random UP textured structures. We demonstrate that the IP structures with their superior AR ability and passivation results have the potential to replace the random UP structures, to further boost the efficiency in SHJ solar cell applications. Finally, the SHJ solar cell with the optimized IP structure exhibits a CE of 14.6% with J_{SC} of 35.3 mA/cm^2, V_{OC} of 605.4 mV, and *FF* of 68.4%.

2. Experimental section

The SHJ solar cells were fabricated using the process illustrated in the flowchart in Fig. S1 in Supporting Information. Random UPs and periodic IPs were fabricated on 4-in. n-type monocrystalline Si Czochralski (001) wafers with a thickness of 200 μm. The random UP structures were obtained by immersing the Si substrates in a potassium hydroxide solution (KOH:IPA:H_2O = 1:1:17) for 20 min at 85 °C. Rectangular arrays with different periodicities were patterned by photolithography using the IP fabrication process. After this, a 30-nm-thick SiO_2 layer was deposited as an etching mask. After the lift-off process, the substrates with patterned SiO_2 layers were immersed in a potassium hydroxide solution (KOH:IPA:H_2O = 1:1:17) at 85 °C. After SiO_2 removal by HF, IP structures with different periodicities were obtained. Subsequently, all patterned substrates were cleaned by the standard RCA process followed by dipping in 1% HF. To fabricate SHJ solar cells, an intrinsic buffer (10 nm)/p-type-doped *a*-Si:H layer (6 nm) were deposited on the front, and an intrinsic buffer (10 nm)/n-type-doped *a*-Si:H layer (10 nm) were deposited on the back by plasma-enhanced chemical vapor deposition (PECVD) at 150 °C. A 92-nm-thick ITO layer was deposited by sputtering on the both sides as a transparent conducting layer. After deposition of the ITO films, the cells were annealed at 210 °C in air for 30 min. Finally, Ag grids were deposited on the both sides by e-beam evaporation.

Morphological studies were carried out using JEOL JSM-6500 field emission SEM. Reflectance measurements were performed by a JASCO V-670 UV–vis spectrometer equipped with an integral sphere. The minority carrier lifetime measurement was analyzed using the quasi-steady-state photoconductance technique (QSSPC) on a Sinton WCT120. The PV performance of the current density-voltage (*J*–*V*) characteristics was monitored under illumination by an air mass (AM) 1.5G solar simulator at 100 mW/cm^2 with a Keithley 2400 source meter. External quantum efficiency (*EQE*) measurements were performed by coupling a Halogen lamp to a monochromator.

3. Results and discussion

Fig. 1a shows the structure of a complete SHJ solar cell. Fig. 1b–d illustrates three kinds of Si surfaces for comparison: polished, random UP, and periodic IP surfaces. The SEM images of the random UP and the periodic IP structures are shown in Fig. 1e and f. Conventional random UPs ranging from 7 to 14 μm in width were fabricated by immersing as-cut Si substrates in an anisotropic etching solution. Some pyramids less than 1 μm in width or half pyramids were also generated between big pyramids (Fig. 1e). It is difficult to obtain a surface with the same size of UPs by only using wet etching, even changing concentration of etching solution, time, or temperature [29]. Pyramids with an angle of 54.7° to the wafer surface formed at a much higher etching rate in the [100] direction than that in the [111] direction due to the higher atomic density in the (111) plane than that in the (100) plane [30]. Large areas of periodic IP structures with different periodicities were obtained by using photolithography technique combined with the anisotropic etching process. Fig. S2a–S2c in Supporting Information show the SEM images of the IP structures with periodicities of 6, 10, and 14 μm, respectively. The sizes of the IPs are controlled by photolithography and etching time. The ridge width of the IP structures is controlled in the range of 1–1.5 μm.

To investigate the light-harvesting abilities of the IP structures, the spectral R_{total} was measured for comparison with substrates with polished and random UP surfaces. Fig. S3 in Supporting Information shows the R_{total} of IP structures with different periodicities to first optimize the IP structures. The IP structure with a 10-μm periodicity exhibits the lowest reflectance over the wavelength range from 300 to 1100 nm. Optical and electrical properties of IP with optimized 10-μm periodicity would be compared with polished and random UP surfaces in the following study. In contrast to polished and UP surfaces, the IP surface reduces the reflectance over the broadband regions and exhibits reduced average R_{total} from 41.2% (polished surface) and 19.2% (random UP surface) to 15.3% (Fig. 2a). The IP surface shows lower R_{total} than the random UP surface because of the superior light–trapping ability of the periodic IP structures. The incident rays bounce multiple times off the pyramidal structures with incident light absorbed during every bounce. The large difference in the size of the UPs is disadvantageous to confining the light within the structures. Moreover, from the simulation, it can be seen that most of the incident rays bounce three times on the walls of the IPs but only twice between the UPs. The increased number of bounces of reflected light in the IPs increases the probability of light absorption [26,27,31]. Furthermore, the light scattered by the structures enters the substrates at oblique angles, increasing the length of the optical path, which is important especially in solar cell application.

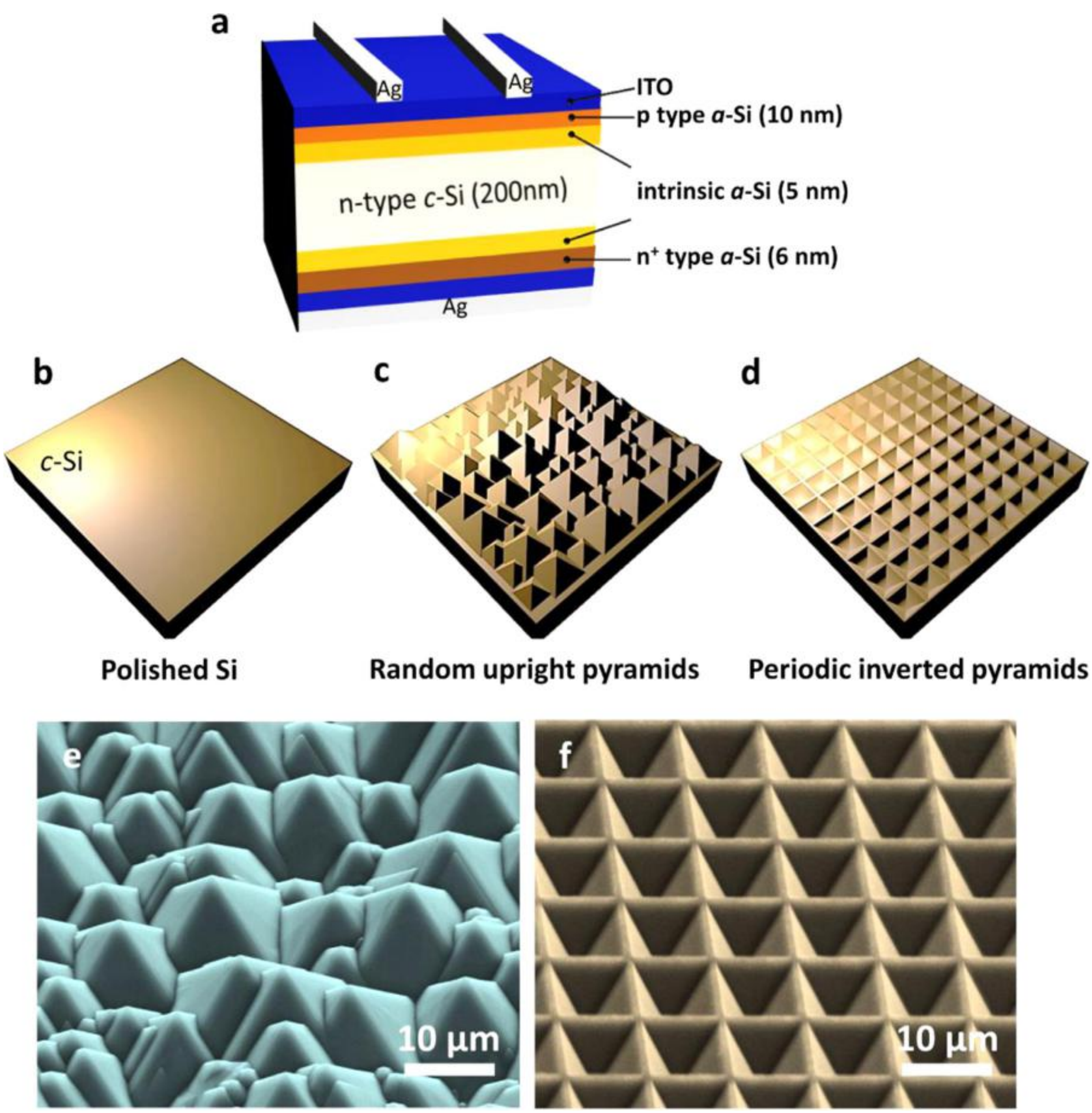

Fig. 1. (a) The device structure of the SHJ solar cells. (b)–(d) Schematics of various surface profiles on the *c*-Si. (e) and (f) 45°-tilted SEM images of the random UPs and periodic IPs with a 10 μm in periodicity.

Fig. 2b shows the R_{total} spectra of the different AR surfaces after the *a*-Si:H/ITO deposition. ITO is commonly used for solar cell applications, serving not only as a transparent conductive electrodes but also an AR layer. According to thin-film interference theory, the R_{total} can be suppressed at specific wavelengths (to almost zero) by adjusting the thickness of the ITO layer. Given that the reflective index of ITO at the wavelength of 650 nm is 1.764, the optimum thickness of ITO to minimize the reflection at the wavelength around 650 nm is 92 nm. It is worth examining the R_{total} of complete devices. Although SHJ solar cells achieve a world-record high V_{OC}, the optical loss from the absorption in *a*-Si (band gap = 1.7 eV) always limits the J_{SC}. Therefore, it is important to improve the AR performance in this range to compensate the optical loss from *a*-Si. Due to AR ITO films, there is a strong decrease in the average reflectance for an IP structure at the wavelengths lower than 730 nm from 22.3% (polished surface) to 6.7%, which is also much lower than that of the random UP structure (8.3%).

The high V_{OC} due to significant passivation by *a*-Si:H is the most important advantage of SHJ solar cells. Efficient energy-harvesting structures not only demonstrate superior light-harvesting ability, but also can well passivate the defective surfaces by depositing ultrathin *a*-Si:H films. The minority carrier lifetime measurement offers a way to examine the effect of passivation. The QSSPC technique provides a simple way to examine the effective minority carrier lifetime (τ_{eff}). The measured τ_{eff} of the total recombination includes surface and bulk recombination. Because the bulk recombination of these samples is the same, the variation of measured τ_{eff} can be considered to the difference in surface recombination rate [32,33]. Fig. 3a shows the carrier lifetime of substrates with different surfaces after being passivated by 5 nm intrinsic *a*-Si:H *via* the PECVD. The IP structure exhibits a higher τ_{eff} than the random UP structure, indicating that the IP structure is well passivated by intrinsic *a*-Si:H through PECVD as compared to the random UP structure. The superior passivation performance on IP structures can be explained by the more uniform a-Si:H coverage for periodic valleys with the same depth rather than random sharp peaks, resulting in a higher V_{OC}, which will discussed below. The substrate with polished surface shows a relatively low τ_{eff} due to the higher surface state density of the (100) plane [34,35].

The implied V_{OC} of the devices, assuming no loss from electrical contact, can be extracted from the excess carrier lifetime measurement

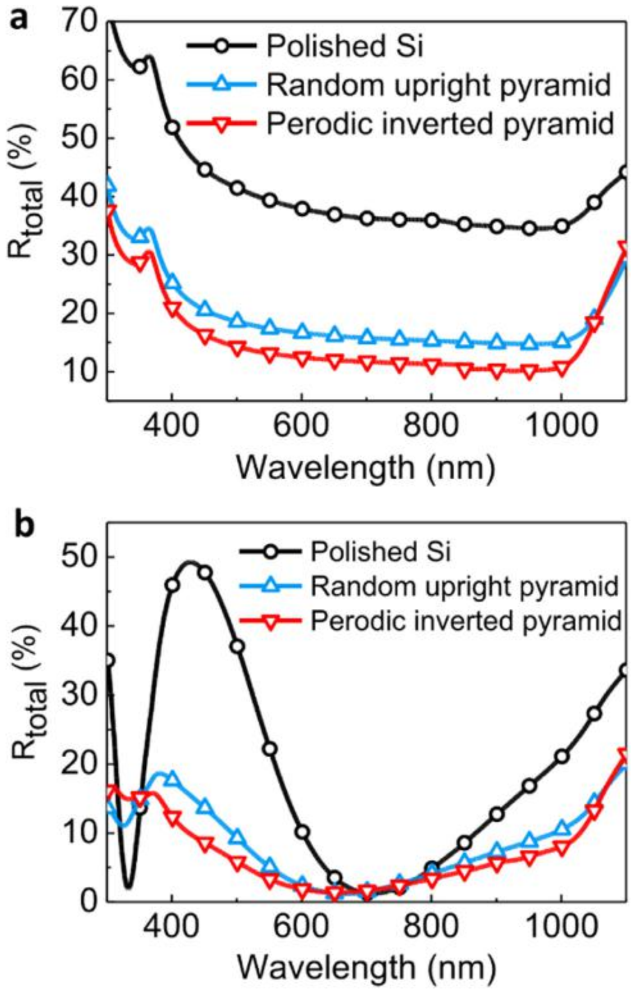

Fig. 2. R_{total} of polished, random UP, and parodic IP textured surfaces (a) without and (b) with the deposited *a*-Si:H/ITO films.

[36]. The implied V_{OC} is estimated from the equation [34]:

$$j_{ph} = \frac{q\Delta n_{av} W}{\tau_{eff}} \quad (1)$$

$$\text{implied } V_{oc} = \frac{kT}{q} \ln\left(\frac{\Delta n \cdot (N_{D,A} + \Delta n)}{n_i^2} \right) \quad (2)$$

where j_{ph} is the photoexcited current, q is the charge of the electron, Δn_{av} is the average density of minority charge carriers, W is the wafer thickness, k is the Boltzmann constant, T is the temperature, $N_{D,A}$ is the donor or acceptor concentration of the wafer, Δn is the excess carrier concentration, and n_i is the intrinsic carrier concentration. Under open-circuit conditions, the recombination current will balance the photoexcited current. Δn_{av} would be similar to the value of Δn when the wafer surface is well-passivated and the wafer thickness is smaller than carrier diffusion length. Then, with a given j_{ph}, implied V_{OC} can be calculated by replacing Δn_{av} with Δn. The results of τ_{eff} for minority carrier density of 10^{15} cm^{-3} and implied V_{OC} are summarized in Fig. 3b. The implied V_{OC} of the IP structure can be as high as 625 mV due to the great passivation done by intrinsic *a*-Si:H.

Fig. 4a shows the *J*–*V* curves of complete SHJ solar cells with different surfaces, and the characteristics are summarized in Table 1. Compared with polished and random UP textured SHJ solar cells, the SHJ solar cell with energy-harvesting IP exhibits a big enhancement in both J_{SC} and V_{OC} due to the enhanced light absorption obtained by optimization of the size of the IP structures and the improved surface passivation which is verified by the lifetime measurement. A maximum CE of 14.58% is obtained with V_{OC} of 604.5 mV, *FF* of 68.4%, and J_{sc} of 35.3 mA/cm^2.

In order to gain insight into the correlation between the improvement of J_{SC} and optical harvesting/carrier collection enhancement, the *EQE* spectra were measured from 350 to 1100 nm, as shown in Fig. 4b. As compared to polished and random UP textured SHJ solar cells, the *EQE* of the solar cells with the periodic IP structure exhibits an enhancement in the broadband wavelength regions, which agrees with the reflection measurement. The enhancement in *EQE* could readily contribute to the J_{SC} enhancement (Table 1). *EQE* is the ratio of the number of photocarriers collected by solar cells to the number of incident photons. To exclude the optical effect, internal quantum efficiency (*IQE*) is extracted from *EQE* and reflectance for investigating the carrier collection efficiency. The carrier recombination strongly affects the *IQE* [34]. Usually solar cells with the defective surfaces show a high surface recombination rate and thus poor *IQE*, limiting J_{SC}, V_{OC}, and overall efficiency. In this study, the IP structures improves the *IQE* by improving defective interfaces to facilitate carrier collection, echoing the results of the effective lifetime measurements (Fig. 3). It is worth pointing out that device fabrication conditions in the present work are not optimized, and thus the PV performance, particularly V_{OC} and *FF*, can be further improved by optimization of the deposition parameters of the stacked intrinsic/doped *a*-Si:H layers and the electrode contacts to reduce series resistance and interface states.

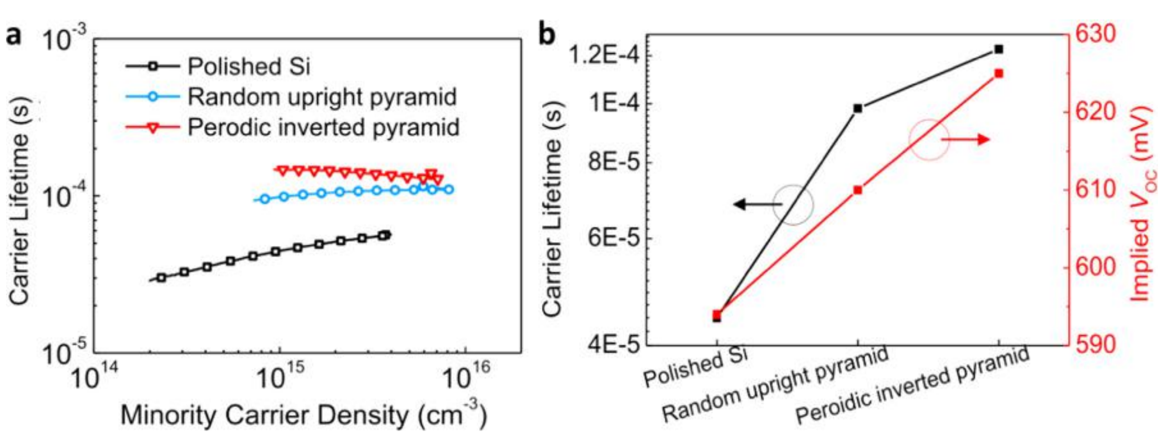

Fig. 3. (a) Minority carrier lifetime as a function of minority carrier concentration for polished, random UP, and parodic IP textured Si substrates after passivation with the 5 nm intrinsic *a*-Si:H layers *via* the PECVD. (b) Lifetimes at a carrier concentration of 10^{15} cm^{-3} and implied V_{OC} for passivation with the intrinsic *a*-Si:H layers.

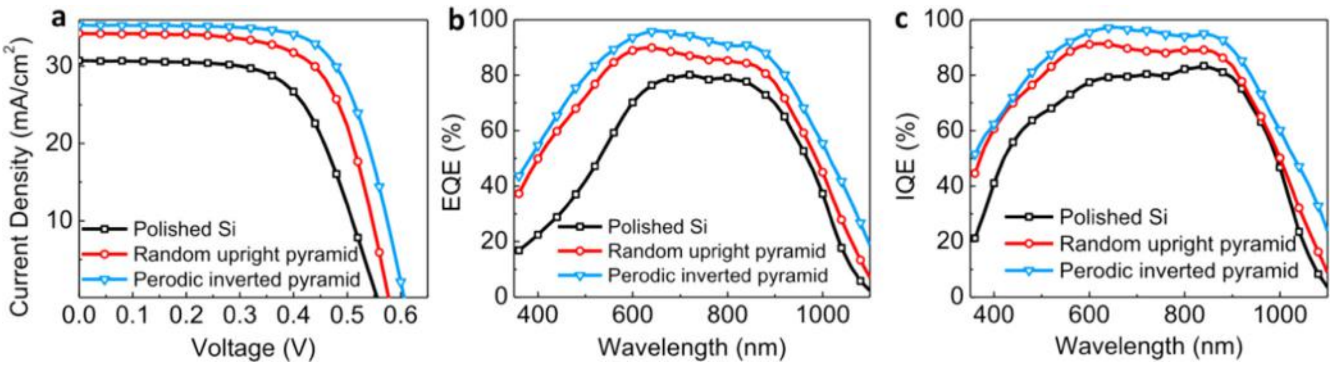

Fig. 4. (a) *J–V* curves, (b) *EQE*, and (c) *IQE* spectra measured for polished, random UP, and parodic IP textured SHJ solar cells.

Table 1
Characteristics of SHJ solar cells with different surface structures.

	V_{OC} (mV)	J_{SC} (mA/cm^2)	*FF* (%)	*CE* (%)
Polished Si	555.8	30.7	62.6	10.4
Random upright pyramid	576.4	34.2	66.8	12.7
Periodic inverted pyramid	604.5	35.3	68.4	14.6

4. Conclusion

We demonstrated that the periodic IP structures have superior harvesting ability and better passivation effect achieved by *a*-Si:H than UP structures. The superiority of the light-trapping properties can be ascribed to a greater portion of the incident light undergoing a triple bounce between the adjacent structures, so that a larger fraction of the light is absorbed before exiting the cell. The increase in minority carrier lifetime shows that superior passivation quality can be obtained by introducing the periodic IP structures due to the more uniform *a*-Si:H coverage for periodic valleys as compared to random sharp peaks of UPs. The improved J_{SC} and V_{OC} of SHJ solar cells with IP textured surface contribute to the significant CE enhancement of 41%, as compared with that offered by a polished surface. The concepts and manufacturing techniques described above would be a viable way to concurrently improve electrical and optical properties for SHJ solar cells.

Appendix A. Supplementary material

Supplementary data associated with this article can be found in the online version at http://dx.doi.org/10.1016/j.nanoen.2016.02.034.

References

[1] H.P. Wang, D.H. Lien, M.L. Tsai, C.A. Lin, H.C. Chang, K.Y. Lai, J.H. He, J. Mater. Chem. C 2 (2014) 3144–3171.
[2] E. Garnett, P. Yang, Nano Lett. 10 (2010) 1082–1087.
[3] B.R. Huang, Y.K. Yang, T.C. Lin, W.L. Yang, Sol. Energy Mater. Sol. Cells 98 (2012) 357–362.
[4] M. Zheng, H.P. Wang, C.M. Sutter-Fella, C. Battaglia, S. Aloni, X. Wang, J. Moore, J.W. Beeman, M. Hettick, M. Amani, W.T. Hsu, J.W. Ager, P. Bermel, M. Lundstrom, J.H. He, A. Javey, Adv. Energy Mater. (2015) 1501337.
[5] J.H. Heo, S.H. Im, J.H. Noh, T.N. Mandal, C.S. Lim, J.A. Chang, Y.H. Lee, H.-j Kim, A. Sarkar, K. NazeeruddinMd, M. Gratzel, S.I. Seok, Nat. Photon. 7 (2013) 486–491.
[6] M.L. Tsai, S.H. Su, J.K. Chang, D.S. Tsai, C.H. Chen, C.I. Wu, L.J. Li, L.J. Chen, J. H. He, ACS Nano 8 (2014) 8317–8322.
[7] W.R. Wei, M.L. Tsai, S.T. Ho, S.H. Tai, C.R. Ho, S.H. Tsai, C.W. Liu, R.J. Chung, J. H. He, Nano Lett. 13 (2013) 3658–3663.
[8] S. Avasthi, S. Lee, Y.L. Loo, J.C. Sturm, Adv. Mater. 23 (2011) 5762–5766.
[9] A. Shah, P. Torres, R. Tscharner, N. Wyrsch, H. Keppner, Science 285 (1999) 692–698.
[10] S. De Wolf, A. Descoeudres, Z.C. Holman, C. Ballif, Green 2 (2012) 7–24.
[11] K. Masuko, M. Shigematsu, T. Hashiguchi, D. Fujishima, M. Kai, N. Yoshimura, T. Yamaguchi, Y. Ichihashi, T. Mishima, N. Matsubara, T. Yamanishi, T. Takahama, M. Taguchi, E. Maruyama, S. Okamoto, IEEE J. Photovolt. 4 (2014) 1433–1435.
[12] M. Taguchi, A. Yano, S. Tohoda, K. Matsuyama, Y. Nakamura, T. Nishiwaki, K. Fujita, E. Maruyama, IEEE J. Photovolt. 4 (2014) 96–99.
[13] H. Angermann, L. Korte, J. Rappich, E. Conrad, I. Sieber, M. Schmidt, K. Hübener, J. Hauschild, Thin Solid Films 516 (2008) 6775–6781.
[14] H.P. Wang, T.Y. Lin, C.W. Hsu, M.L. Tsai, C.H. Huang, W.R. Wei, M.Y. Huang, Y. J. Chien, P.C. Yang, C.W. Liu, L.J. Chou, J.H. He, ACS Nano 7 (2013) 9325–9335.
[15] M. Edwards, S. Bowden, U. Das, M. Burrows, Sol. Energy Mater. Sol. Cells 92 (2008) 1373–1377.
[16] Z. Jiang, Y. Dou, Y. Zhang, Y. Zhou, F. Liu, M. Zhu, J. Semicond. 30 (2009) 084010.
[17] D.Y. Jeong, C.S. Kim, J.Y. Song, J.C. Lee, J.S. Cho, S.H. Park, J.S. Wang, K.H. Yoon, J. Song, Proceedings of the 34th IEEE Photovoltaic Specialists Conference (PVSC), 2009, p. 000642–000645.
[18] L. Fesquet, S. Olibet, J. Damon-Lacoste, S. De Wolf, A. Hessler-Wyser, C. Monachon, C. Ballif, Proceedings of the 34th IEEE Photovoltaic Specialists Conference (PVSC), 2009, p. 000754–000758.
[19] K.V. Maydell, E. Conrad, M. Schmidt, Prog. Photovoltaics Res. Appl. 14 (2006) 289–295.
[20] D.L. King, M.E. Buck, Proceedings of the 22th IEEE Photovoltaic Specialists Conference (PVSC), 1991, p. 303–308.
[21] D. Iencinella, E. Centurioni, R. Rizzoli, F. Zignani, Sol. Energy Mater. Sol. Cells 87 (2005) 725–732.
[22] H. Sai, Y. Kanamori, K. Arafune, Y. Ohshita, M. Yamaguchi, Prog. Photovolt. Res. Appl. 15 (2007) 415–423.
[23] J. Oh, H.C. Yuan, H.M. Branz, Nat. Nanotechnol. 7 (2012) 743–748.
[24] B. Stegemann, J. Kegel, M. Mews, E. Conrad, L. Korte, U. Stürzebecher, H. Angermann, Energy Procedia 38 (2013) 881–889.
[25] J. Zhao, A. Wang, M.A. Green, F. Ferrazza, Appl. Phys. Lett. 73 (1998) 1991–1993.
[26] J. Zhao, M.A. Green, IEEE Trans. Electron Devices 38 (1991) 1925–1934.
[27] A.W. Smith, A. Rohatgi, Sol. Energy Mater. Sol. Cells 29 (1993) 37–49.
[28] J. Zhao, A. Wang, P. Altermatt, M.A. Green, Appl. Phys. Lett. 66 (1995) 3636–3638.
[29] E. Forniés, C. Zaldo, J.M. Albella, Sol. Energy Mater. Sol. Cells 87 (2005) 583–593.
[30] L.L. Kazmerski, Renew. Sustain. Energ. Rev. 1 (1997) 71–170.
[31] Y. Yang, M.A. Green, A. Ho-Baillie, H. Kampwerth, S. Pillai, H. Mehrvarz, Sol. Energy Mater. Sol. Cells 115 (2013) 42–51.
[32] A. Cuevas, D. Macdonald, Sol. Energy 76 (2004) 255–262.
[33] R.A. Sinton, A. Cuevas, Appl. Phys. Lett. 69 (1996) 2510–2512.
[34] H.P. Wang, T.Y. Lin, M.L. Tsai, W.C. Tu, M.Y. Huang, C.W. Liu, Y.L. Chueh, J.H. He, ACS Nano 8 (2014) 2959–2969.
[35] H. Angermann, W. Henrion, A. Röseler, M. Rebien, Mater. Sci. Eng. B 73 (2000) 178–183.
[36] W.G.J.H.M. van Sark, L. Korte, F. Roca, Physics and Technology of Amorphous-Crystalline Heterostructure Silicon Solar Cells, Springer-Verlag: Heidelberg, Germany, 2012, pp. 180–181.

Miss Hsin-Ping Wang received her M.S. degree (2011) in the Graduate Institute of Photonics and Optoelectronics at National Taiwan University, Taipei, Taiwan. She is now a Ph.D. student in Dr. Jr-Hau He's group and currently works in UCSD and UC Berkeley as a visiting scholar. Her research interests include theoretical and experimental research on optical properties analysis of nanostructure, varied types of solar cells, and solar water splitting cells.

Mr. An-Cheng Li received his M.S. degree (2012) in the Graduate Institute of Photonics and Optoelectronics at National Taiwan University, Taipei, Taiwan. His research interests include the periodic inverted pyramid-textured Si heterojunction solar cells, theoretical and experimental research on fabrication of the Si solar cells by using the nano/microscale hierarchical structures to boost the photovoltaic performances, and optical properties analysis and photovoltaic application of nanostructures.

Miss Tzu-Yin Lin received her M.S. degree (2013) in the Graduate Institute of Photonics and Optoelectronics at National Taiwan University, Taipei, Taiwan. She joined Dr. Jr- Hau He's group in 2011. Her research areas include theoretical and experimental research on optical properties analysis of hierarchical structures and varied types of solar cells.

Professor Jr-Hau He received his B.S. and Ph.D. degrees from the National Tsing Hua University, Hsinchu, Taiwan, in 1999 and 2005, respectively. He is currently an Associate Professor of Electrical Engineering program, King Abdullah, University of Science and Technology (KAUST), Kingdom of Saudi Arabia. He is involved in the design of new nanostructured architectures for nanophotonics and the next-generation nanodevices, including photovoltaics, and resistive memory